Elnaz Esmizadeh, Ghasem Naderi*, Sahar Arezoomand and Saeedeh Mazinani

Fabrication and characterization properties of polypropylene/polycarbonate/clay nanocomposites prepared with twin-screw extruder

DOI 10.1515/secm-2015-0406
Received October 13, 2015; accepted April 13, 2016; previously published online June 23, 2016

Abstract: Polypropylene/polycarbonate (PP/PC) nanocomposites containing various proportions of the organically modified montmorillonite were prepared by extrusion and injection molding process. The morphology of PP/PC nanocomposites was characterized by transmission electron microscopy (TEM), scanning electron microscopy (SEM), and X-ray diffraction (XRD). The nanocomposites with 3 or 5 wt% of nanoclay (NC) show a uniform dispersion of the NC as pointed out by two different methods, TEM and XRD. It was shown that the morphology of dispersed phase (PC) is highly dependent on the content of minor phase, which was correlated with the balance of drop breakup and coalescence. The mechanical properties have been investigated by tensile test and Izod impact test. The virgin PP/PC samples showed a reduction in impact strength and elongation at break and up to 50% increase in Young's modulus by increase in PP content comparing with the pure PP. Investigating the effect of NC and PC content on the mechanical behavior of PP/PC nanocomposites showed increased Young's modulus and decreased impact strength with increasing PC and NC loading. An obvious ductile to brittle behavior transition at a high content of PC or NC was supported by notched Izod impact strength experiments and SEM results.

Keywords: extrusion; nanocomposite; polypropylene; organoclay; polycarbonate.

***Corresponding author: Ghasem Naderi,** Faculty of Processing, Iran Polymer and Petrochemical Institute (IPPI), PO Box 14965-115, Tehran, Iran, e-mail: G.naderi@ippi.ac.ir
Elnaz Esmizadeh: Department of Polymer Science and Technology, University of Bonab, PO Box 5551761167, Bonab, Iran
Sahar Arezoomand and Saeedeh Mazinani: Department of Polymer Engineering, South Tehran Branch, Islamic Azad University, Tehran 1777613651, Iran

1 Introduction

Heat deflection temperature (HDT), impact strength, and stiffness of polypropylene (PP) are inferior in comparison with most engineering plastics. There are some different approaches to modify these properties, including blending with another polymer or incorporation of various fillers [1].

Blending of two polymers is a useful way to upgrade the properties of each individual component. Polycarbonate (PC) as an engineering plastic having outstanding mechanical properties and heat resistance has been reported to upgrade PP's performance. PP/PC is an incompatible and immiscible blend because of the significant difference in the flow characteristics of two polymers [1]. A great number of studies based on PP/PC blends are reported in literature [2–8]. Dobrzański et al. [4] showed that polymer PP/PC blends processed by melt manipulation techniques show improved modulus compared with neat PP. Also, the effect of compatibilizer (glycidyl methacrylate) on the morphological, thermal, rheological, and mechanical properties of PP/PC blends were investigated by Zhihui et al. [5]. The significant improvement in HDT at high PC content in PP/PC has been reported by Liang et al. [6]. The comprehensive studies by Favis et al. showed that viscosity ratio, composition, and processing parameters control the morphology and mechanical properties of the PP/PC blend [9–14].

Reinforcing polymer matrix with various fillers continues to be one of most important methods to create new materials with improved mechanical, thermal, and physical properties [15, 16]. The effects of PC addition in red mud (RM)-filled PP on the rheological properties of PP showed that the addition of PC in RM-filled PP reduced its shear stress and melt viscosity [1]. Montmorillonite clays are known as very effective fillers in polymeric matrices because of the opportunity to get materials with improved mechanical properties, barrier properties, and resistance to thermal degradation at low loadings. This is due to

Table 1: The properties of polymer matrix components and NC.

	Condition	Unit	Value
PP			
Melt flow index (MFI)	230°C/2.16 kg	g/10 min	3.5
Rockwell hardness	R-Scale	–	100
Vicat softening point	1 kgf	°C	152
Heat deflection temperature (HDT)	4.6 kg/cm^3	°C	104
Density	23°C	g/cm^3	0.9
Tensile modulus	ISO 527/23°C	MPa	1400
Izod impact strength	ASTM D256	J/m	25
PC			
Melt flow index (MFI)	230°C/1.2 kg	g/10 min	1.2
Glass transition Temperature (T_g)	10°C/min	–	145
Vicat softening point	10 N	°C	145
Heat deflection temperature (HDT)	1.8 MPa	°C	125
Density	23°C	g/cm^3	1.2
Tensile modulus	ISO 527/23°C	MPa	2400
Izod impact strength	ASTM D256	J/cm	9.60
Cloisite 15A			
Cation exchange capacity (CEC)	–	mEq/100 g	125
Aspect ratio	–	–	75–100
Density	23°C	g/cm^3	1.66

the platelet-like (layered) structure of these nanofiller in combination with the high aspect ratio, which enables significant improvement of properties at low filler concentrations if good dispersion of filler in polymer matrix is ensured [17, 18].

Polymer nanocomposites based on nanoclay (NC) and polymer blend matrix have been widely investigated by our group [19–23], but up to our knowledge, there is no sufficient quantitative data published on nanocomposites based on the PP/PC blend. In the present work, an analysis of the morphology and mechanical properties of PC/PP nanocomposites prepared by melt blending method is presented, and the effect of different weight fractions of PC and NC were incorporated on the final properties of PP is discussed.

2 Experimental

2.1 Materials

The commercial-grade iso-tactic PP homopolymer (SEETEC H5300) used in this study was supplied by LG chemical Co., South Korea. PC, Makrolon® 2858, was purchased from Bayer Co, Germany. Cloisite 15A, natural montmorillonite modified with a quaternary ammonium salt (dimethyl, dehydrogenated tallow ammonium), was obtained from Southern Clay Products, USA [24]. Details of the materials used in this study are given in Table 1.

2.2 Preparation of nanocomposites

PC, PP, and NC particles were kept in an air circulating oven at 100°C for 24 h for drying before being used to minimize hydrolytic degradation. The nanocomposite samples were compounded according to the formulations presented in Table 2 using a twin-screw extruder. The extruder was a corotating, intermeshing, self wiping, with a modular 2-cm screw and an L/D ratio of 40 (Brabender, Germany). Screw speed was kept constant at 75 rpm. All the components were mixed mechanically and then fed to the extruder. Temperatures of feed, compressive, metering zones, and die was fixed between 255°C and 260°C.

Table 2: Sample codes and compositions.

Sample code	PP (wt%)	PC (wt%)	Cloisite 15A (wt%)
P90C10N0	90	10	0
P85C15N0	85	15	0
P80C20N0	80	20	0
P70C30N0	70	30	0
P87C10N3	87	10	3
P85C10N5	85	10	5
P83C10N7	83	10	7
P80C10N10	80	10	10
P80C15N5	80	15	5
P75C20N5	75	20	5
P65C30N5	65	30	5
P100C0N0	100	0	0

Continuous strands obtained from the die of the extruder were granulated after cooling in a cold-water bath. The extruded pellets were injection molded into standard mechanical test sample molds using an injection-molding machine (ENGEL, Denmark) after drying in a vacuum oven at 80°C for 20 h. The temperature in the injection-molding machine was kept at 180°C and 240°C from hopper to die. The mold temperature was fixed 40–50°C, and the injection pressure was 100 bar.

2.3 Physical and mechanical analysis

To investigate the performance of polymer components under thermal conditions of processing, thermogravimetric analysis (TGA) was conducted under atmospheric conditions with a heating rate of 5°C/min. Tensile test was conducted on dumbbell-shaped specimens obtained from injection molding according to ASTM D638 by tensile testing machine (Instron 8511, UK) with a crosshead separation speed of 50±10 mm/min. An impact Izod Tester (Zwick 5102, Germany) was used at room temperature to measure the impact resistance of the samples according to ASTM D256.

2.4 Morphological analysis

The dispersion state of layered silicates is analyzed by small angle X-ray scattering (SAXS). X-ray diffraction (XRD) data are collected on a Philips X'Pert PRO (The Netherlands) with a CuK radiation of wavelength of 1.54 Å using an accelerating voltage of 40 kV. Diffraction spectra are obtained over a 2θ range of 2°–10°, and the interlayer spacing (d_{001}) is calculated using the Bragg's equation, $d_{001}=\lambda/2\sin\theta_{max}$, where λ is the wavelength and d_{001} is the interlayer spacing of silicate layers. Scanning electron microscopy (SEM) was performed using a scanning electron microscope (Tescan VEGA-II, USA) after a gold sputtering of 100–500 Å. PC part was extracted from the cryofractured surface with selective extraction method using chloroform. Choloroform is a suitable solvent for PC/PP blend because of its inability to swell or penetrate through the PP [17]. The phase structure of PC/PP/NC was examined by a Philips (Netherlands) CM120 transmission electron microscopy (TEM) using an acceleration voltage of 120 kV. The ultrathin sections were cut from the injection-molded samples by ultra-microtome equipped with a diamond knife (approximately 100 nm thick) in liquid nitrogen.

3 Results and discussion

3.1 TGA analysis

To investigate the thermal stability of polymer components in the process described previously, thermogravimetric examination was performed in the air for PC and PC.

Figure 1 illustrates the results of TGA tests performed in the air; both mentioned polymers show single-stage degradation. The figure shows that the degradation of PP started at 260°C while that of PC started at 370°C. The onset temperatures of the degradation of these samples indicate that the temperature range of processing is not risky because a slight or no thermodegradation is expected.

3.2 PP/PC blends

To evaluate the mechanical properties and morphology of PP/PC composites, two categories of samples were prepared. First, PP and PC were blended together at different PC contents without any nanofiller as reference samples; second, PP was blended with PC in the presence of various amounts of NC. The former set is discussed in the next section.

To determine the quality of the blends structure, PP/PC samples were examined by a scanning electron microscope. SEM images of the blends with 10 and 30 wt% PC are shown in Figure 2. A complex variation was observed in the morphology of dispersed phase (PC) in injection-molded samples by increasing PC content.

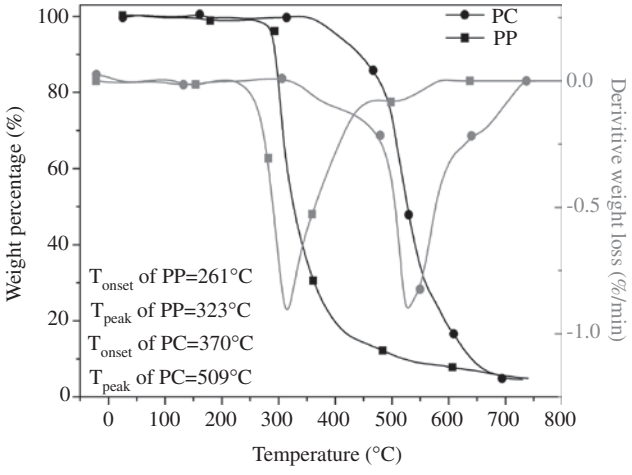

Figure 1: Effect of temperature on weight change (TGA plot of virgin PP and PC).

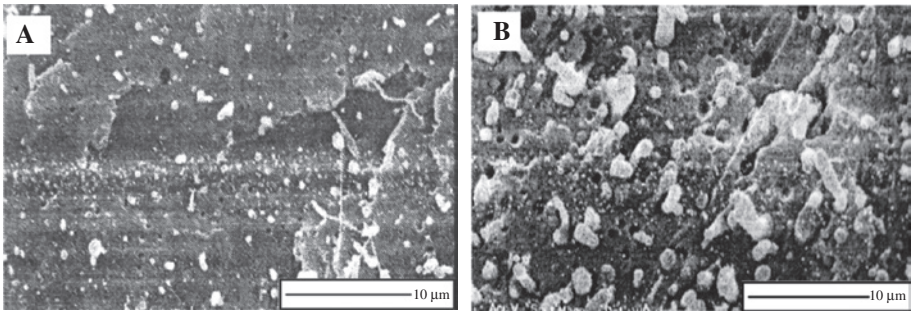

Figure 2: SEM micrographs of cryofractured surfaces of PP/PC blends. (A) Blend with 10 wt% PC, (B) blend with 30 wt% PC.

At low PC content (sample with 10 wt% of PC), the minor phase mostly takes up spherical and elliptical shape (Figure 2A). At high PC content (sample with 30 wt% of PC), the spherical domains of minor phase have enlarged and, in some cases, elongated into cylinder-like formation (Figure 2B). The droplet size of the minor phase in polymer blends obtained from melt blending process depends on a balance of two principal forces, normal forces and surface tension forces, which are related to two individual phenomenon, drop breakup and coalescence, respectively [25]. Furthermore, it is generally believed that the size of the dispersed phase escalates by increasing the composition due to the greater possibility of phase contacts and particle-particle interactions. This would occur until particle-particle interactions develop into sufficiently pronounced state results in formation of extended structures [13]. This observation is consistent with the morphological studies conducted with Favis et al. [26]. Differences between the morphology of dispersed phase in PP/PC blends shown in Figure 2 can be attributed to the lower viscosity of the PC compared with PP matrix. With the increase of PC, the dispersed phase particles will get bigger so they can be more easily deformed by the shear and elongational stresses exerted to the sample during the mold filling [26]. It is also observed that the size of the cavities grows with increasing PC concentration. This can be attributed to high interfacial tension (low interfacial adhesion) between two polymer phases. It was shown that the interfacial tension measured for PC imbedded in a PP matrix using the breaking thread method varies from 17.3 mN/m at 225°C to 13.8 mN/m at 265°C [27].

Figure 3 presents Young's modulus and elongation at break for the entire PP/PC blend molded by injection molding. On the basis of mechanical test, it was found that the increment of PC content in the PP/PC blend, as a rigid phase, causes the increment of Young's modulus values. Moreover, the cylindrical shape of minor phase in high content PC samples can significantly improve the mechanical properties [11]. Reverse behavior was observed

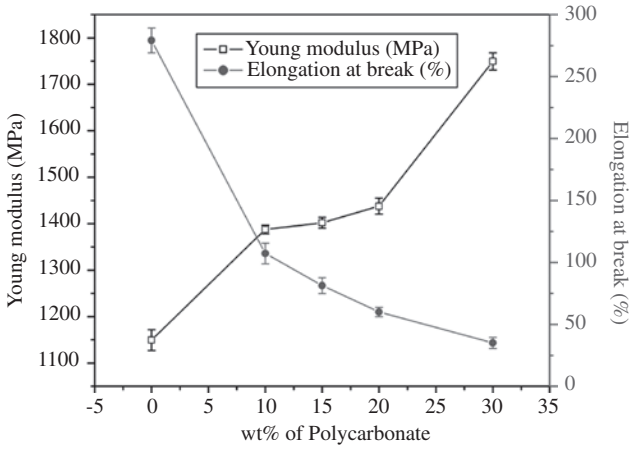

Figure 3: Young's modulus and elongation at break of PP/PC blends.

for elongation at break, where the increment of PC content results in a decrement of elongation at break. The incorporation of PC into the PP matrix, as a rigid phase, hinders the ability of the material to yield. In addition, the big droplet size of PP and the weak adhesion between PP and PC phases result in crack formation in interface leading to low elongation at break [28]. In all amounts of PC, the fracture of the blend occurs in a ductile manner during the tensile test. These observations are in agreement with those of Dobrzański et al. (2008), which was attributed to the increase of flexural modulus of PP/PC having higher PC percentage [4].

The elongated morphology (cylindrical shape) of the PC domains caused by the addition of PC content is believed to be the result of an increase in impact strength. By contrast, the reduction in interfacial adhesion of separated phases leading to poor transfer of exerted energy or force from one phase to another results in dropping impact strength [29]. Impact results in Figure 4 indicate that the positive effect of cylindrical morphology of PC on impact strength can be significantly suppressed by a weak interface between PP and PC phases at a high content of PC.

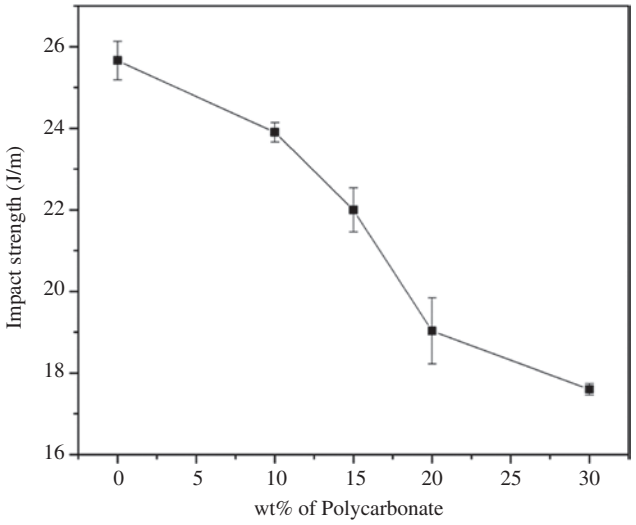

Figure 4: Effect of PC content on notched Izod impact strength of PP/PC blends.

3.3 PP/PC nanocomposites

The dispersion of the NC layers in the PP/PC matrix was examined by XRD, calculating the clay interlayer spacing d_{001} from the 2θ position of the clay (001) diffraction peak using Bragg's law.

Figure 5 shows the series of X-ray diffraction spectra of original Cloisite15A and PP/PC/Cloisite15A composites. The interlayer spacing (d_{001}) of Cloisite15A calculated from Bragg's equation is 29.52 Å, recalling that the characteristic peak occurred at 2θ=2.99°. For all nanocomposite samples with 10 wt% of PC (Figure 5A), the XRD pattern exhibits a shift of peak to lower angles, indicating an increase in the interlayer spacing of NC. This indicates that the polymeric chains can intercalate into the interlayer of NC. The results of θ of the characteristic peak and related interlayer spacing are summarized in Table 3. The interlayer spacing decreases progressively, from 32.34 Å for 3 wt% NC to 31.08 Å for 10 wt% NC. However, in the range of high amounts of NC, no significant increase in interlayer spacing is observed compared with virgin Cloisite 15A. The observed broadening of peaks and the reduction in intensity can be assumed as the sign of more disordered stacks of layered silicates while maintaining their periodic structure [30].

Figure 5B shows that in all blend composition, interlayer spacing is somewhat higher than the values of virgin Cloisite 15A. The XRD diffraction pattern of PP/PC nanocomposites with various concentrations of PC (see Figure 5B) reveals that increasing PC content from 10 to 30 wt% reduces the interlayer spacing of NC layers. This observation suggests that a significant portion of the PC

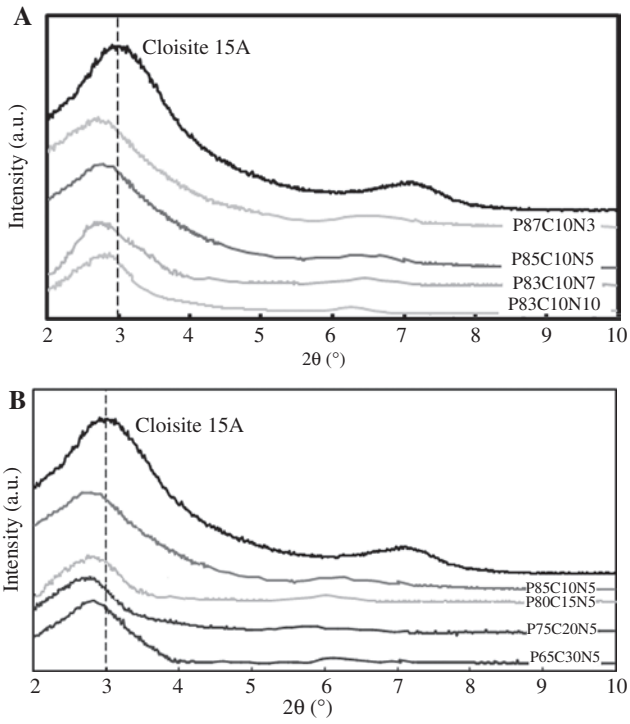

Figure 5: XRD patterns of PP/PC nanocomposites in which (A) The concentration of dispersed phase (PC) kept constant and equal to 10 wt% and (B) the concentration of NC (Cloisite 15A) kept constant and equal to 5 wt%.

Table 3: SAXS-derived $2\theta_{max}$ and related *d*-spacing for PP/PC nanocomposites.

Sample code	$2\Theta_{max}$	d_{001}
Cloisite 15A	2.99	29.52
P87C10N3	2.73	32.34
P85C10N5	2.77	31.87
P83C10N7	2.81	31.41
P80C10N10	2.84	31.08
P80C15N5	2.79	31.64
P75C20N5	2.80	31.53
P65C30N5	2.81	31.30

matrix cannot intercalate into the gallery space of layered NC. In fact, the interlayer spacing seems to be confined, most likely an outcome of the decreased melt viscosity and exerted shear tension with increase in PC content. This is in good agreement with previously published data on the PP/PC blends [1].

To confirm the intercalation of polymeric chains into the gallery space of NC, TEM experiment was conducted. The dispersion state of NC is given in Figure 6 in which the dark lines are the cross-section of Cloisite 15A layers, the lighter areas belong to PC region, and the lightest areas are related to PP region (according to related density).

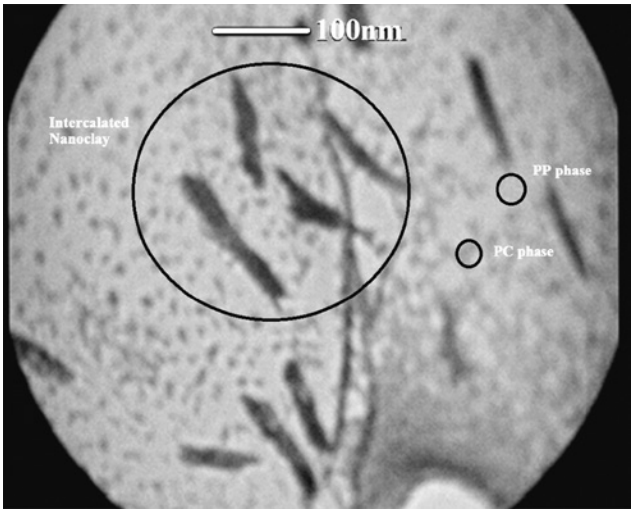

Figure 6: TEM image of PP/PC nanocomposites with 10 wt% PC and 5 wt% NC.

TEM result for the PP/PC nanocomposites are agree well with XRD measurements, which suggested that intercalated morphology was obtained during mixing process.

The SEM micrographs of the fracture surface of PP/PC nanocomposites after PC extraction are given in Figure 7. As shown, the surfaces of the studied PP/PC nanocomposites appeared rough compared with that of virgin PP/PC blend. The observed phenomenon can be attributed to improved interaction between the two phases in the presence of NC. On the other hand, it is well known that microsized agglomerates increase in size with increasing NC content and can change fracture mode from ductile to brittle deformation [31, 32]. Therefore, it would be expected that the large amount of NC can act as stress concentration sites, leading to much less fracture resistance [33]. It is worth to note that when PC content increases, the nature of the fractured surface changes

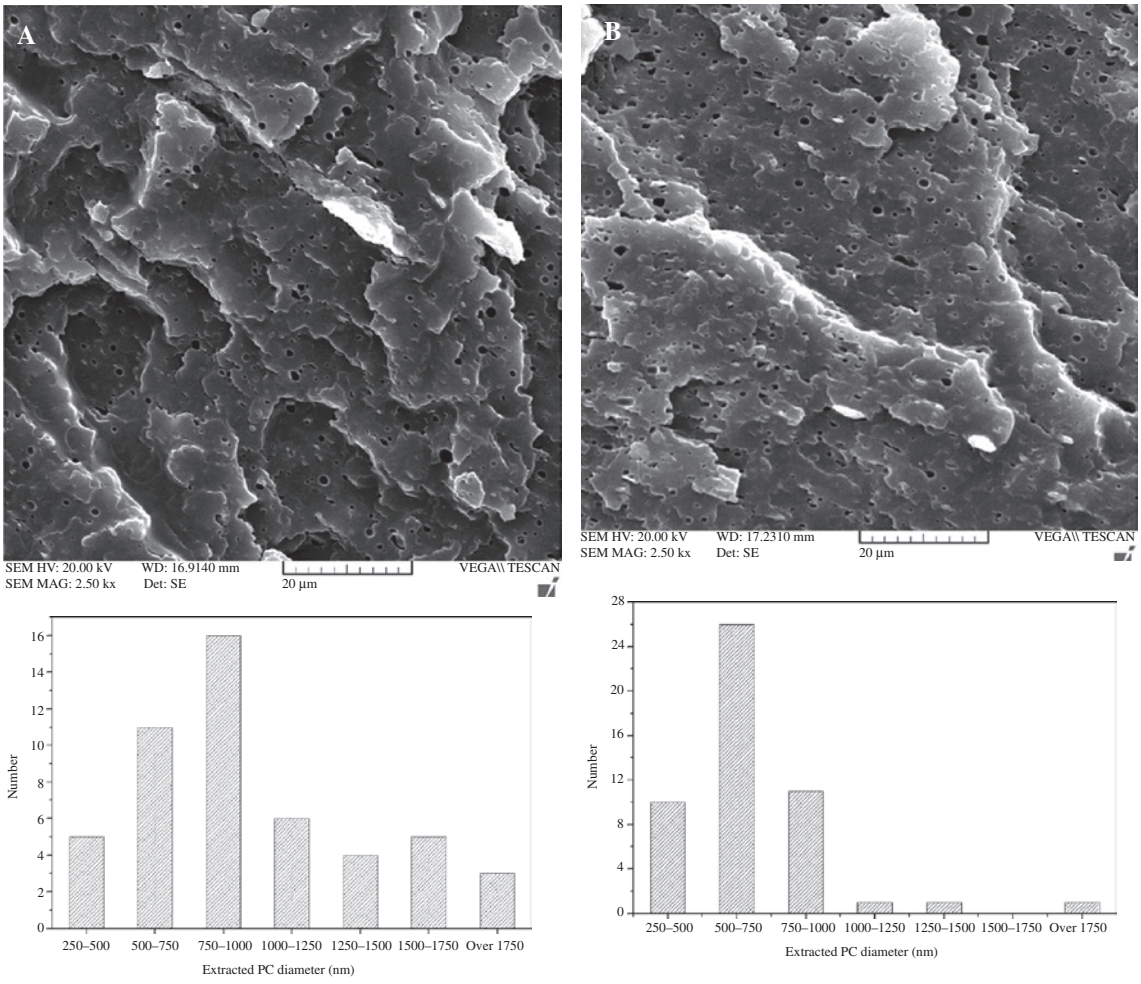

Figure 7: SEM micrographs of cryofractured surfaces of PP/PC nanocomposites after PC extraction: (A) Nanocomposite with 10 wt% PC and 5 wt% NC, (B) nanocomposite with 10 wt% PC and 10 wt% NC, (C) nanocomposite with 30 wt% PC and 5 wt% NC.

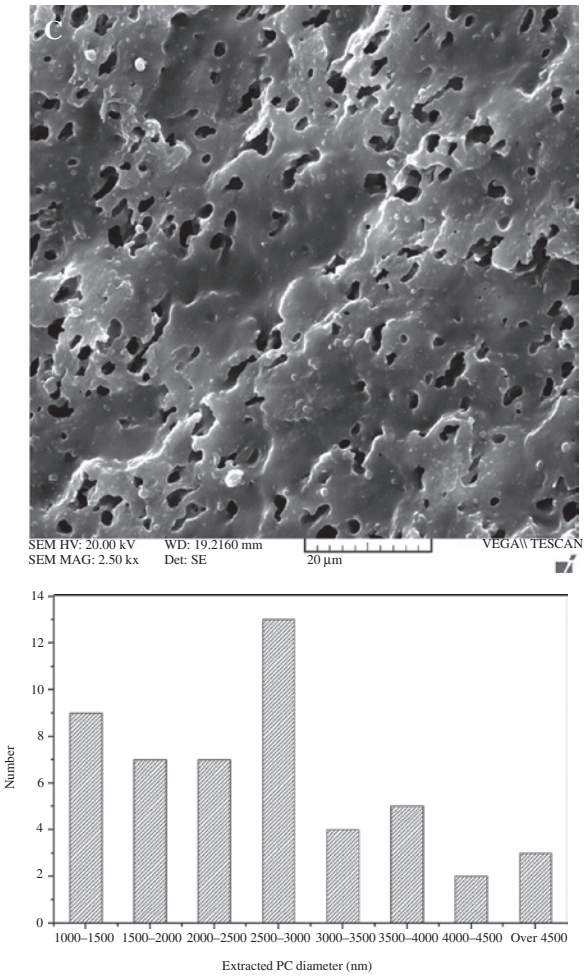

Figure 7 (continued)

from rough to smooth. This is due to the higher proportion of the low viscosity phase (PC) and the correlated low shear tension exerted to the sample [34]. The voids observed in the figure have been related to PC domains extracted during etching process. Furthermore, as can be seen in Figure 7, the introduction of NC results in very small spherical-shaped domains of PC, which are uniformly distributed throughout the entire fracture surface. The related histograms showed that with increasing NC, the peak of the diagram shifts to the smaller diameters. In the other words, the number of the extracted PC particles with a diameter of 750–1000 nm was maximum in the case of P80C10N5 sample, whereas the maximum was observed at the extracted PC particles with a diameter of 500–750 nm in the case of P80C10N10 sample. This observation can be related to the fact that NC addition increases the shear tension and the melt viscosity of polymers, prompting the possibility of droplet breakup, which was reported in our previous work [35]. Even at low NC content (Figure 7A and C), there is a significant effect of NC on the size distribution of PC phase.

The effects of NC filler and PC concentration on the tensile properties of PP/PC nanocomposites in terms of Young's modulus and elongation at break are shown in Figure 8. Comparing the Young's modulus of PP/PC nanocomposites with results of virgin PP/PC demonstrates that Young's modulus increases when nanocomposites are formed (Figure 8A). Such behavior is the direct result of reinforcing the effect of intercalated or stacked NC. Not only nanodispersion including intercalation and exfoliation determines mechanical behavior of nanocomposites, but also microdispersion has a great influence. Microparticles can initiate failure caused by stress concentration at high NC content [31, 36]. For the nanocomposite containing 3 and 5 wt% NC, the significant increase in Young's modulus was observed, whereas for further amounts of NC, improvement gradually decreases. This well agrees with the decrease of intercalation for the nanocomposites

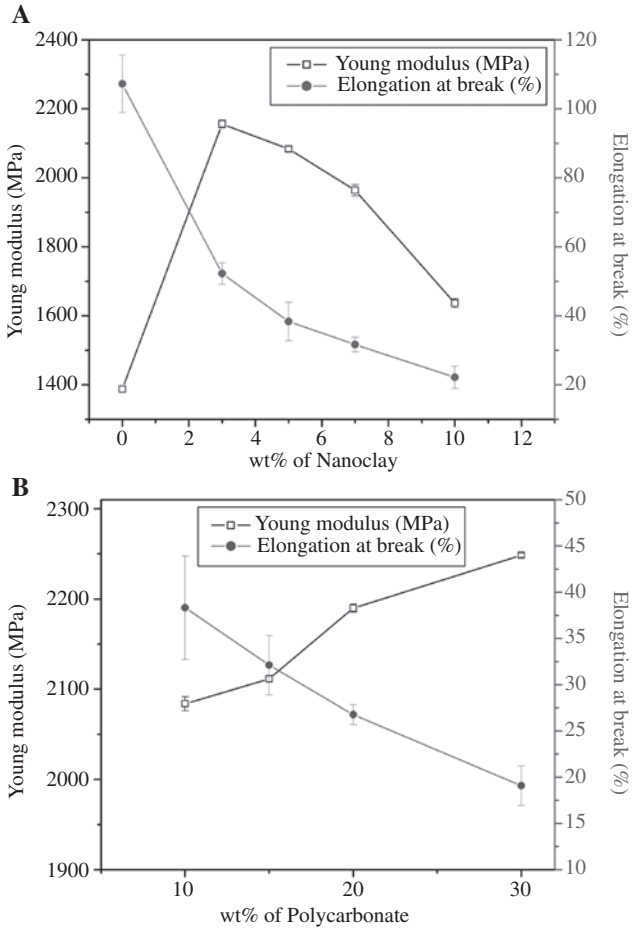

Figure 8: Young's modulus and elongation at break of PP/PC nanocomposites: (A) Effect of NC content, (B) effect of PC content.

containing more than 5 wt% of NC (detected at XRD results). The brittle mode fracture shown in SEM results again verifies the microdispersion existence in nanocomposites with high amounts of NC. The mechanical behavior of the PP/PC nanocomposites with increasing PC concentration at a constant amount of NC (Figure 8B) is reminiscent of that of virgin blend. A significant enhancement in Young's modulus compared with that of virgin PP/PC was observed in all concentration of PC, as illustrated in Figure 8B. Tensile test results show that at high filler or PC loadings, ductility is reduced, which can be indicated by a significantly lower elongation at break for both. The observed mechanical results are similar to those reported in the literature [31, 32, 36].

Reduced ductility concluded from elongation at break data is also evident in Izod notched impact test results.

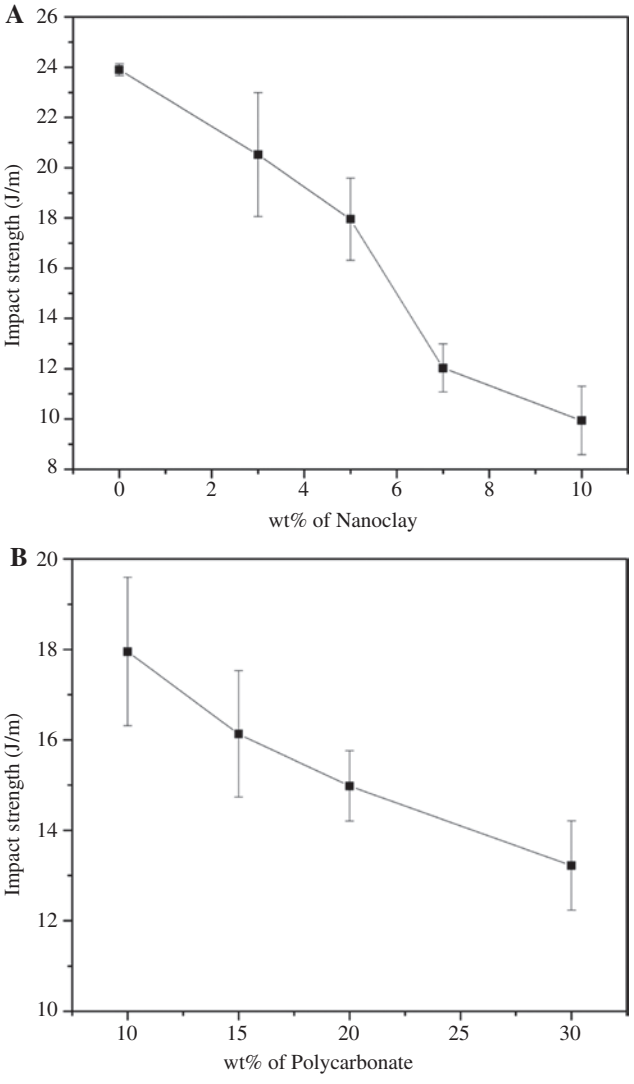

Figure 9: Izod impact strength at break of PP/PC nanocomposites: (A) Effect of NC content, (B) effect of PC content.

The variations of impact resistance in PP/PC nanocomposites with PC and NC contents are presented in Figure 9. To summarize the behavior, it can be noted that the increment at a weight percent of PC or NC causes the decrement of impact strength.

4 Conclusion

A new PP/PC/organomodified clay nanocomposite with an intercalated morphology of the NC layers has been prepared by melt processing in twin-screw extruder. X-ray diffraction patterns and TEM micrographs confirm the intercalation of the polymer chains between the NC layers. The addition of the NC particles slightly decreases the particle size of disperse phase (PC) compared with the neat PP/PC blend. The Young's modulus is increased in the presence of the NC. Furthermore, the new nanocomposite shows a higher Young's modulus by increasing the PC concentration of the blend.

Impact strength analysis and SEM results confirm the brittle fracture behavior of nanocomposites at more than 5 wt% NC because of the stress concentration phenomenon. This weak mechanical performance, i.e. gradual decrease in Young's modulus at more than 5 wt% of NC, is attributed to the coalescence of the NC, which prevents tension transfer between two polymer phases. Brittle manner was observed with increasing PC content because of the decreased ease of movement of polymer chain segments in the PP/PC nanocomposite.

References

[1] Chand N, Hashmi S. *Bull. Mater. Sci.* 1999, 22, 801–804.
[2] Pillai PKC, Narula GK, Tripathi AK, Mendiratta RG. *Phys. Rev. B.* 1983, 27, 2508–2514.
[3] Pillai P, Narula G, Tripathi A, Mendiratta R. *J. Appl. Phys*. 1982, 53, 6953–6955.
[4] Dobrzański L, Król M, Bilewicz M, Viana J. *J. Achieve. Mater. Manuf. Eng.* 2008, 27, 19–22.
[5] Zhihui Y, Xiaomin Z, Yajie Z, Jinghua Y. *J. Appl. Polymer Sci.* 1997, 63, 1857–1863.
[6] Liang Z, Williams HL. *J. Appl. Polymer Sci*. 1991, 43, 379–392.
[7] Pillai P, Narula G, Tripathi A. *Jpn. J. Appl. Phys*. 1984, 23, 1251–1257.
[8] La Mantia FP. *Mater. Chem. Phys*. 1987, 16, 115–123.
[9] Fisa B, Favis B, Bourgeois S. *Polym. Eng. Sci.* 2004, 30, 1051–1055.
[10] Favis BD, Chalifoux JP. *Polym. Eng. Sci.* 1987, 27, 1591–1600.
[11] Favis BD, Chalifoux JP. *Polymer* 1988, 29, 1761–1767.

[12] Favis BD, Willis JM. *J. Polym. Sci. B. Polym. Phys.* 1990, 28, 2259–2269.
[13] Favis B, Therrien D. *Polymer* 1991, 32, 1474–1481.
[14] Favis BD. *Can. J. Chem. Eng.* 2009, 69, 619–625.
[15] Jafari SH, Asadinezhad A, Vahid AK, Khonakdar HA, Wagenknecht U, Heinrich G. *Polym. Plast. Technol. Eng.* 2012, 51, 682–688.
[16] Vahidifar A, Nouri Khorasani S, Park CB, Naguib HE, Khonakdar HA. *Ind. Eng. Chem. Res.* 2016, 55, 2407–2416.
[17] Pötschke P, Kretzschmar B, Janke A. *Compos. Sci. Technol.* 2007, 67, 855–860.
[18] Golebiewski J, and Galeski A. *Compos. Sci. Technol.* 2007, 67, 3442–3447.
[19] Esmizadeh E, Naderi G, Ghoreishy MHR. *J. Appl. Polymer Sci.* 2013, 130, 3229–3239.
[20] Akhlaghi S, Sharif A, Kalaee M, Elahi A, Pirzadeh M, Mazinani S, Afshari M. *Mater. Des.* 2012, 33, 273–283.
[21] Esmizadeh E, Naderi G, Ghoreishy MHR, Bakhshandeh GR. *Iran Polym. J.* 2011, 20, 587–596.
[22] Naderi G, Lafleur PG, Dubois C. *Polym. Eng. Sci.* 2007, 47, 207–217.
[23] Azizli MJ, Naderi G, Bakhshandeh GR, Soltani S, Askari F, Esmizadeh E. *Rubber. Chem. Technol.* 2014, 87, 10–20.
[24] Southern Clay Products I, http://www.scprod.com/.
[25] Gonzalez-Nunez R, De Kee D, Favis B. *Polymer* 1996, 37, 4689–4693.
[26] Fisa B, Favis BD, Bourgeois S. *Polym. Eng. Sci.* 1990, 30, 1051–1055.
[27] Chapleau N, Favis BD, Carreau PJ. *Polymer* 2000, 41, 6695–6698.
[28] Srinivasan KR, Gupta AK. *J. Appl. Polymer Sci.* 1994, 53, 1–17.
[29] Shayuti MSM, Abdullah MZ, Yusoff PSMM. Compressive properties and morphology of polypropylene/polycarbonate blends. In *Proceedings of International Conference on Environment and Industrial Innovation (ICEII 2011)*. 2011.
[30] Lertwimolnun W, Vergnes B. *Polymer* 2005, 46, 3462–3471.
[31] Nevalainen K, Vuorinen J, Villman V, Suihkonen R, Järvelä P, Sundelin J, Lepistö T. *Polym. Eng. Sci.* 2009, 49, 631–640.
[32] Hsieh AJ, Moy P, Beyer FL, Madison P, Napadensky E, Ren J, Krishnamoorti R. *Polym. Eng. Sci.* 2004, 44, 825–837.
[33] Chan C-M, Wu J, Li J-X, Cheung Y-K. *Polymer* 2002, 43, 2981–2992.
[34] Akhtar S, De P, De S. *Mater. Lett.* 1988, 6, 186–190.
[35] Esmizadeh E, Naderi G, Barmar M. *Fiber. Polym.* 2014, 15, 2376–2385.
[36] Gonzalez I, Eguiazabal J, Nazabal J. *Polym. Eng. Sci.* 2006, 46, 864–873.